The use of very high resolution images for studying Posidonia oceanica reefs

A. Tomasello, F. P. Cassetti, A. Savona, V. Pampalone, M. Pirrotta, S. Calvo, G. Signa, C. Andolina, A. Mazzola, S. Vizzini, et al.

VIE ET MILIEU - LIFE AND ENVIRONMENT, 2020, 70 (3-4): 25-35

THE USE OF VERY HIGH-RESOLUTION IMAGES FOR STUDYING *POSIDONIA OCEANICA* REEFS

A. TOMASELLO[1], F. P. CASSETTI[1], A. SAVONA[1], V. PAMPALONE[1], M. PIRROTTA[1], S. CALVO[1], G. SIGNA[1,2], C. ANDOLINA[1,2], A. MAZZOLA[1,2], S. VIZZINI[1,2], A. MUZIRAFUTI[3], S. LANZA[3], G. RANDAZZO[3]*

[1] *Dipartimento di Scienze della Terra e del Mare (DiSTeM), Università degli Studi di Palermo, Italy*
[2] *CoNISMa, Consorzio Nazionale Interuniversitario per le Scienze del Mare, Rome, Italy*
[3] *Dipartimento Scienze Matematiche ed Informatiche, Scienze Fisiche e Scienze della Terra (MIFT), Università degli Studi di Messina, Italy*
** Corresponding author: federicapaola.cassetti@unipa.it*

SEAGRASS
UPPER LIMIT
DRONE
3D MODEL
DEAD *MATTE*
CARBON SINK
UAVS
ATOLL

ABSTRACT. – *Posidonia oceanica* is an endemic Mediterranean seagrass that forms wide and dense meadows from the surface up to about 40 m depth. This species can develop a biogenic structure called *matte*, a typical terraced formation built up by itself, consisting of intertwined rhizomes, roots and sediment, which may allow shoots to reach the sea surface forming reefs (*récif barrière*), considered natural monuments. *Posidonia oceanica* reefs are particularly exposed to the ongoing increase in temperature and in storm frequency and intensity due to climate change, with negative repercussions on their conservation. Much more attention must be paid to the implementation of monitoring tools able to detect early signs of reef regression. In this study, the distribution of *P. oceanica* reefs located along southern coasts of Sicily (Italy, Mediterranean Sea) was investigated. A remote sensing approach was used to assess reef extension, morphological features (*e.g.*, atolls), upper limit and occurrence of dead *matte*. In particular, very high-resolution drone images (~ 2 cm pixel size), combined with GPS field data, were used for 2D- and 3D-reconstruction of *P. oceanica* reefs. The 3D-model allowed to estimate bathymetrical distribution of *P. oceanica* reef enabling to achieve a more detailed and complete understanding of the *P. oceanica* reef architecture.

INTRODUCTION

The dominant and endemic Mediterranean seagrass *Posidonia oceanica* (Linnaeus) Delile is a long-lived species that forms extensive meadows and grows from nearly the water surface to depths up to 40 m (Mazzella & Buia 1986). It constitutes a "climax" community and its presence attests to a relatively stable environment (Francour *et al*. 1999, Montefalcone *et al*. 2008). *Posidonia oceanica* meadows play a pivotal role in numerous ecological and geomorphological key processes such as nutrient recycling, provision of food for fauna, shelter and nursery areas for many species, sequestration of carbon, stabilization of sediment, attenuation of waves through their canopy (Mazzella *et al*. 1992, Mateo *et al*. 1997, Buia *et al*. 2000, Hemminga & Duarte 2000, Vizzini 2009). *Posidonia oceanica* can grow on different substrates including sand, which is easily penetrable by the roots, rocks, in which crevices host the very sturdy roots, and *matte*, a unique terraced biogenic structure formed by the entanglement of roots, rhizomes and sediment (Jeudy de Grissac & Boudouresque 1985). *Posidonia oceanica* can adapt the direction of its growth (horizontally or vertically) to the rate of sediment deposition. Under sedimentation, rhizomes grow vertically (orthotropic growth) to avoid burying (Molinier & Picard 1952, Caye 1980, 1982, Boudouresque & Meinesz 1982) resulting in *matte* edification. In sheltered and shallow water this process can lead to the *matte* rise up, with the leaf tips over, close to the sea surface and subsequent formation of a reef-made barrier (*récif barrière sensu* Boudouresque & Meinesz 1982). Reefs can persist for century or millennia and are increasingly considered as "natural monuments" (Calvo 1987, Pergent *et al*. 2007, 2014, Bonacorsi *et al*. 2013, Boussard *et al*. 2019) and their census is still in progress (Rouanet *et al*. 2019). Both natural and anthropogenic disturbances may endanger *P. oceanica* reefs. These structures are particularly threatened by temperature rise (Tomasello *et al*. 2009, Pergent *et al*. 2014) and erosion caused by sea storms (Short & Neckles 1999, Boudouresque *et al*. 2012), which are expected to increase in intensity due to climate change (IPPC 2019). Furthermore, erosion leads to the exposure and then oxidation of the carbon accumulated within the *matte*, causing the shift of the reefs from sinks to sources of carbon (Boudouresque *et al*. 2016). The stability of these structures along the Mediterranean coasts has been evaluated showing different results, since they have been observed in regression (Boudouresque *et al*. 1975, Tomasello *et al*. 2009, Pergent *et al*. 2014), or in progression (Bonacorsi *et al*. 2013). To gain a better understanding of the actual state of *P. oceanica* reefs, much more attention should be paid to the

implementation of monitoring tools able to detect the first signs of reef regression (Pergent *et al*. 2014). Improving our knowledge of these particular biogenic structures is of pivotal importance to check their status, given that the available maps used to estimate their changes do not constitute a reliable baseline because of their low accuracy (Bonacorsi *et al*. 2013). Recently, the use of very high-resolution images acquired by Unmanned Aerial Vehicles (UAVs) has increased markedly in the field of remote sensing of the environment, due to their advantages in terms of lightweight and low cost required allowing to work at an appropriate spatial and temporal scale needed to study ecologically relevant variables (Anderson & Gaston 2013). Over the past decade, UAVs have been widely used for terrestrial studies, consequently enhancing, as technological developments rapidly advance, their versatility and functionality so much that their use has opened new opportunities such as monitoring of sensitive marine habitats (Ventura *et al*. 2018). Currently, UAVs are able to define also the 3D-reconstruction of an object or scene through a high number of photographs taken from different points of view (Figueira *et al*. 2015). Very recently, they have also been tested for seabed mapping with particular reference to marine vegetation (Duffy *et al*. 2018, Ventura *et al*. 2018), showing a very promising potential. The aim of this study was to test the use of UAVs (drone) images for evaluating the distribution of *P. oceanica* reefs located along the Southern coast of Sicily (Italy, Mediterranean Sea). In this framework, we used photogrammetry obtained by UAVs to analyze reef features and their bathymetrical distribution.

MATERIALS AND METHODS

Study area: The study was carried out in June 2019 along the Southern coast of Sicily (Italy), within the site of European community importance "Fondali Di Capo San Marco-Sciacca" (cod. ITA040012) (Fig. 1). Straight beaches, with medium fine sands mostly quartzy, interspersed with cliffs that subtend, rather irregularly, several small pocket beaches, characterize the geomorphology of the site. The cliff behind, about 5 m high, is mainly composed of sandy clay deposits from the Upper Pliocene - Middle Pleistocene, and is dominated by a terrace of the Tyrrhenian Sea. At the foot of the cliff there are sand – gravelly deposits, very irregular, protected by little protruding promontories, but above all by cobbles (64-256 mm) and boulders (> 256 mm) widely present in the coastal area immediately in front; these deposits are to be linked to the erosion of the cliff, being different from those present in the neighboring areas in terms of granulometry, composition and color. Within the site, *P. oceanica* forms several reefs along the coast (Fig. 1). In particular, six main reefs are present almost continuously distributed along about 2 km, forming a lagoon-like environment with the co-occurrence of other two seagrasses, *Cymodocea nodosa* (Ucria) Ascherson and *Zostera noltei* Hornemann (Perzia *et al*. 2011). Rarely, *P. oceanica* grows at few meters far from the shoreline (about 3 m), forming a *récif frangeant* (Boudouresque & Meinesz 1982). In this study, the reef located in front of the

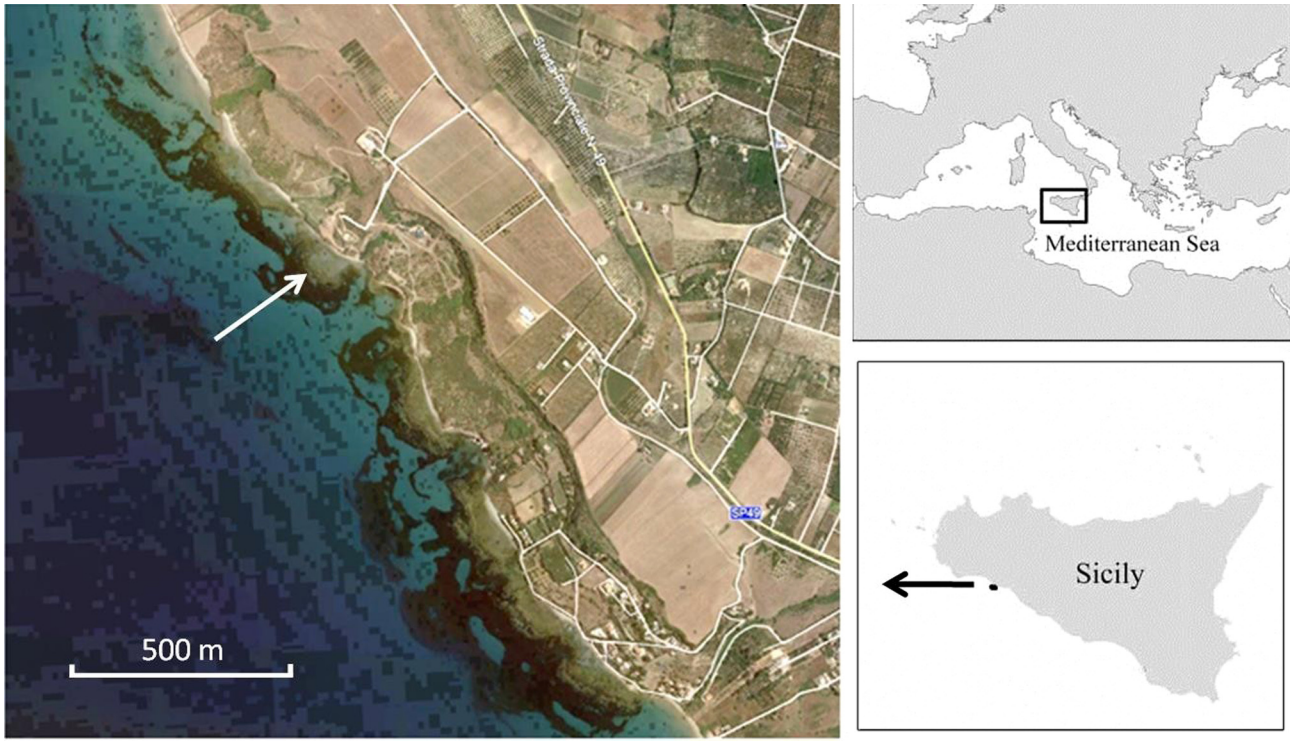

Fig. 1. – Study area with indication of the Maragani's reef.

location "Maragani", was investigated (Fig. 1). The reef is settled mainly on rock resulting in processes of collapse and retreat due to causes connected to the same intrinsic instability of the cliff system (lithological and geomorphological) and to the subsurface hydraulic circulation typical of the coastal stretch. The material crushed by the cliff remained on site incorporated within the interior of the meadow. The reef attenuates wave energy (Fig. 2), determining the formation of a small lagoon-like area characterized by a very shallow depth (< 1 m), low hydrodynamism, seabed with dead *matte*, muddy sediment and rare and very scattered rock blocks. Within the lagoon, water exchange is guaranteed by tidal oscillations and / or breaking waves that pump water inside the lagoon from which they come out through small lateral channels within the reef (AT personal observation).

Data acquisition: Two types of aerial images acquisition were performed in the area: one flight was carried out at a height allowing a resolution enough to avoid photo-interpretation errors, while the other one was carried out at a higher resolution to estimate bathymetry.

In particular, the first type of acquisition was performed by using a DJI Mavic Pro UAV (743 g take-off weight) for assessing seagrass distribution. The drone was equipped with a 12 Mpx camera (CMOS sensor) with a focal length of 4.73 mm to collect 98 calibrated photos each covering an area about 40 × 30 m. The flight height was 30 m, which, as demonstrated by Casella *et al*. (2017), is suitable to depict shallow water characteristics, reaching a ground sample distance (GSD) of ~ 1 cm/pixel according to the following formula:

$$GSD_{cm/pix} = [(Sw_{mm} \times Fh_{m}) / (Fl_{mm} \times Iw_{pix})] \times 100$$

where GSD is the photo resolution on the ground, Sw is the sensor width, Fh is the flight height, Fl is the focal length of the camera, and Iw is the image width (Ventura *et al*. 2018). The flight time was 11 minutes. In this case, the overlap of the images was 60 %, while sidelap was ~ 30 % for a total ~ 1.6 ha of sea recorded.

For the second flight a DJI Mavic 2 UAV (~ 907 g take-off weight) was used for image acquisition to estimate bathymetry. The drone was equipped with a 20 Mpx camera (CMOS sensor) with a focal length of 10 mm to collect 102 calibrated images covering the same area as the former flight (1.6 ha) where a single photo covers an area of about 80 × 50 m. The flight height was 65 m (GSD = 1.52 cm/pix) and a flight time of 7 minutes. The overlap and sidelap of the images for the bathymetry esti-

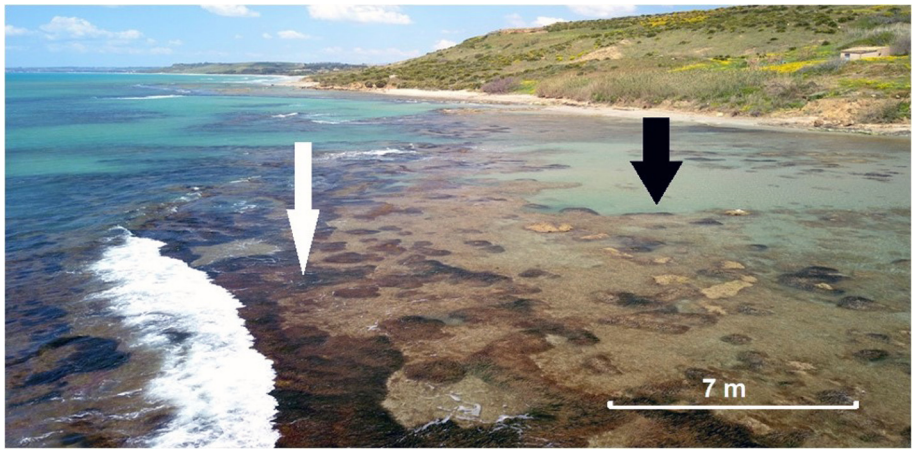

Fig. 2. – The waves break on the reef (white arrow). The black arrow points the small lagoon behind.

Fig. 3. – The flight plan with the sequence of image shot.

Fig. 4. – Target positioning with Topcon HiPer HR.

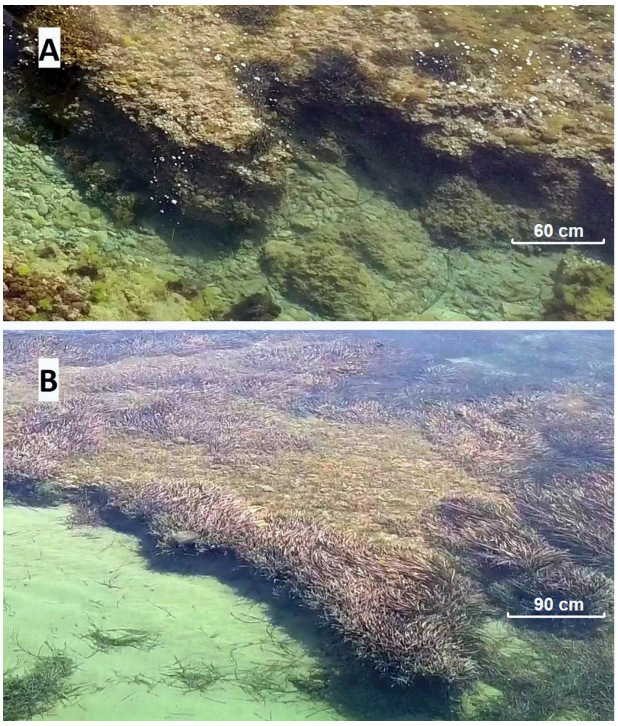

Fig. 5. – Aerial images of *matte* wall detected on the outer (**A**) and inner (**B**) side of the reef in a close-up perspective view obtained by drone flying at few meters above the sea.

mation were ~ 75 % (Fig. 3). In both cases the angle of the camera was set at 90° (to collect nadiral images). Take-off and landing were controlled manually by an operator on the field through a remote control. A Global Navigation Satellite System (GNSS) Topcon HiPer HR (horizontal and vertical error 5 mm + 0.5 ppm and 10 mm + 0.8 ppm, respectively) was also used to detect 11 landmarks on the field (five underwater and six on land) as control points using quadrangular targets 50 x 50 cm size (Fig. 4). One control point acquired on the beach/sea interface was used to rescale all elevation of the other points. Further 16 control points, set as 0 hydrometric, were also chosen directly in the images in correspondence of *Posidonia* leaves that clearly emerged at different points at the time of flight. Both surveys were carried out on same morning characterized by calm sea conditions and clear sky.

Data processing:

2D mosaic

The realization of the 2D mosaic of the *P. oceanica* reef along Maragani coast involved the use of Image Composite Software (ICE 2.0), an advanced panoramic image stitcher (https://www.microsoft.com/en-us/research/product/computational-photography-applications/image-composite-editor/), which allowed to create 2D high-resolution scenarios from a set of overlapping photographs. More specifically, the images of the 30 m flight were imported into the software and a structured serpentine panorama was set, selecting the initial photo and the direction to follow, emulating the programmed flight plan.

Bathymetry

The aerial photographs were analyzed with an appropriate software (Pix4D – https://support.pix4d.com/hc/en-us) that uses advanced SfM (Structure for Motion) and multi-view stereo (MVS) algorithms to construct an ortho-photomosaic and a 3D point cloud from overlapping photographs. The software is capable of automatic identification of key points on all photos, bundle adjustment, point cloud densification, mesh building and texturing (Casella *et al*. 2017, Marre *et al*. 2019). In a first step, the photographs were aligned by means of SfM algorithms identifying image feature points and then the movement of those points throughout the image data set was monitored (~ 180,000 points). The software also calculated the relative camera positions at the moment of image acquisition and internal calibration parameters. Secondly, a dense point cloud was built obtaining ~ 40,000,000 points. Thirdly, the geometric details were built through the analysis of the pixel values operated by the algorithms. It is a sophisticated procedure based on an advanced computer vision solution that enables the creation of high-quality 3D-content from a series of overlapping images. Then, the mesh was textured with photographs. The SfM approach requires a set of points of known coordinates (ground control points) that measures the difference between true coordinates and its coordinates calculated from all photos, to compute pixel-to-earth transformations and to georeference the data point cloud. From the point cloud, the software generated an orthorectified photomosaic with a resolution of 1.49 cm/pix and a DEM with a resolution of 5.95 cm/pix. Finally, the orthophotos and DEMs were exported from Pix4D and imported into a GIS software (Quantum GIS). The distortion resulting from the air-water interaction in the final DEM was corrected through the Snell's law by multiplying the cells in the submerged areas by the refractive index of water (1.34), assuming a planar water

surface unaffected by waves or surface rippling, and integrating these values into the original DEM (Woodget *et al*. 2015, Agrafiotis *et al*. 2020). A sub sample of DEM points was then regressed *vs* the control points set acquired in field by GPS.

3D Model

The last step was to construct a 3D model of the reef. In particular, the 2D photomosaic obtained with the 30 m flight was georeferenced using, as a base, the orthophoto derived from the flight performed at 65 m. The high-resolution georeferenced image was then re-projected directly on the 3D-surface (Rende *et al*. 2015). In this way, an excellent level of detail was reached still maintaining the ability to identify unequivocally *P. oceanica* meadow in a 3D vision. Then some meadow morphologies were digitalized in order to record upper limit bathymetrical position and *matte* elevation. The upper limit was traced on patches longer than 5 m and facing toward the lagoon, maintaining always a distance of 5 cm from the leaves, in order to measure the bathymetrical position of the seabed on which shoots were settled thus avoiding to erroneously record the top level of canopy. Moreover, other morphologies were also analyzed. In particular, dead *matte* walls previously noted during field activities (Fig. 5) were recognized on the photomosaic first and then their thickness was measured on the corresponding 3D model. These measures were finally compared with those recorded *in situ*.

RESULTS

Meadow distribution

Generated photomosaic of the reef, obtained by the flight at 30 m, showed very clearly the distribution of *P. oceanica* meadow (Fig. 6), since it was possible to recognize the leaves of the seagrass in the whole image (Fig. 7). The high level of transparency combined with shallow water allowed to detect important features of the sea bottom. In particular, on the right side of the area, proceeding from North to South, *P. oceanica* meadow is interspersed with an extensive sandy glade, among them it shows a wide band with an almost continuous coverage. Southernmost, the meadow deviates to east until reaching the coast. Inside the meadow several rocky blocks mainly in the southernmost part are present (Fig. 8). Proceeding towards the coast, the meadow becomes progressively more fragmented near its upper limit where the reef emerges with leaves up to the surface also forming

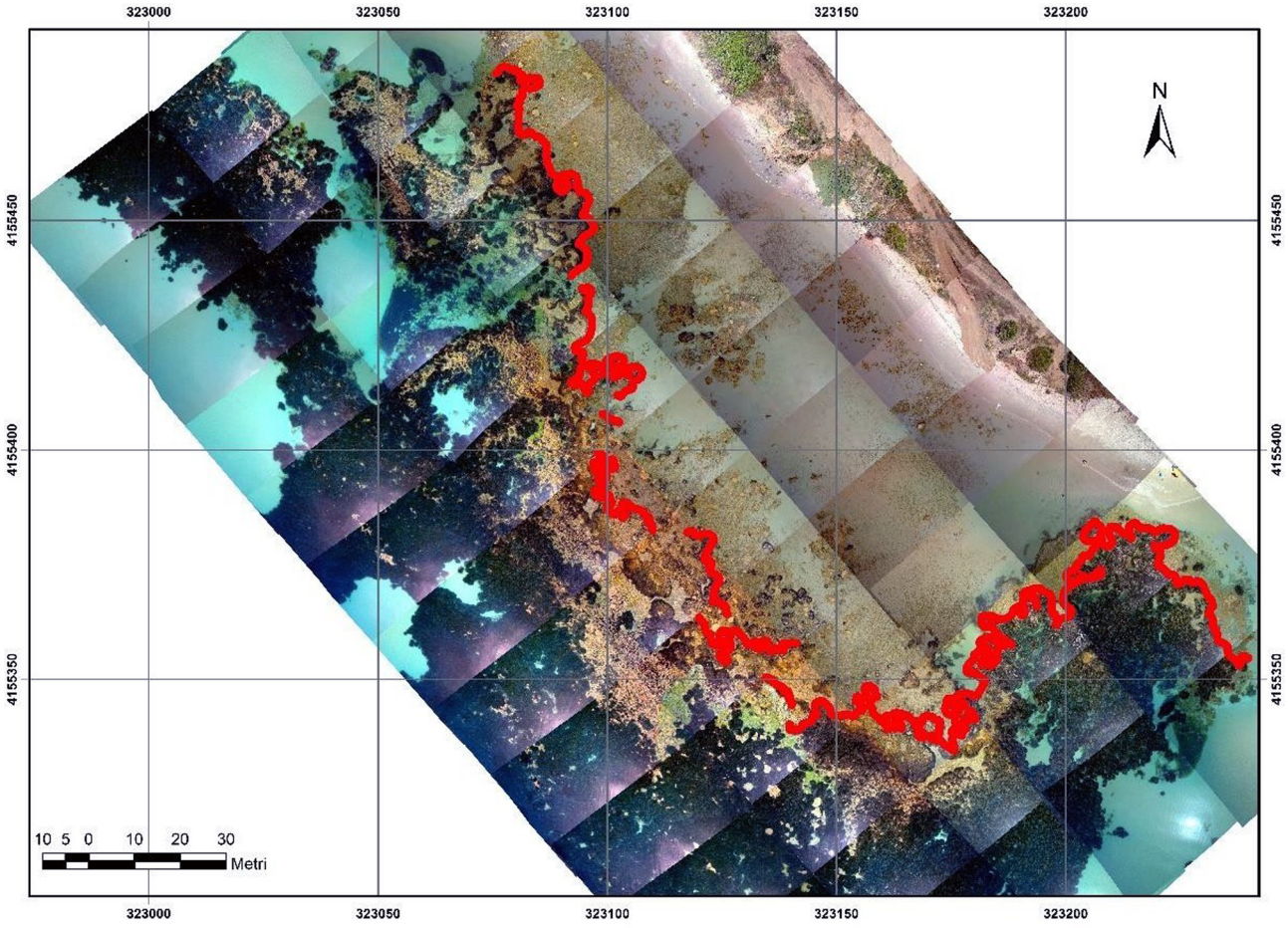

Fig. 6. – Reef photomosaic with *P. oceanica* upper limit over-imposed.

atoll-like patches more or less arched and surrounded by dead *matte* (Fig. 9). The atoll structures have an average diameter that oscillates between 1.27 m and 5.26 m, showing an irregular shape sometimes elongated with the presence of multiple arches on the perimeter. The inner dead *matte* showed variable sizes, resulting in an average thickness of the live atoll ring ranging from 0.24 m to 3.85 m. Patches composed predominantly by living shoots occurred densely grouped in the South-Eastern sector of the reef, very close to the coast (Fig. 10). Inside the reef small rocky blocks, grouped or alone mixed with sporadic patches of *P. oceanica* are also found.

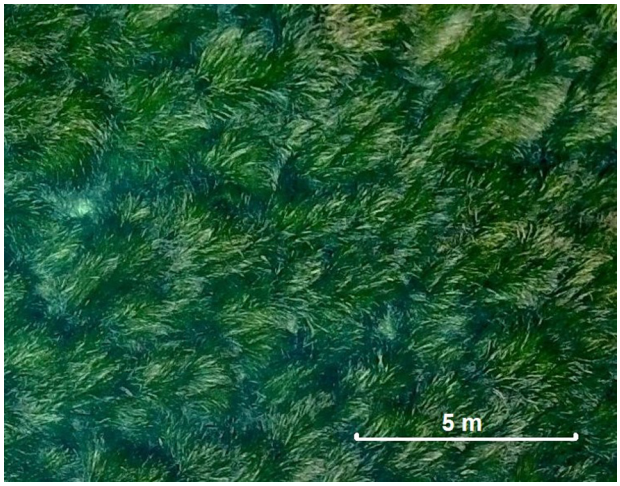

Fig. 7. – Continuous *P. oceanica* meadow. The leaves, more or less covered by epiphytes (lighter), can be distinguished.

Fig. 8. – Several emerging rocky blocks can be identified within or outside the meadow.

Bathymetric map

The DEM generated through the images acquired with flight height of 65 m allowed to obtain the bathymetric map of the area. Regression between control and estimated bathymetrical points extracted from DEM showed a linear agreement on average (Fig. 11). The map shows bathymetry ranging from 0 to 2.31 m (Fig. 13).

A rising seabed coincides with the reef platform, which has an average depth of $-0.13 \pm 1\times10^{-5}$ m. Two depressions in the area behind the reef were detected. Particularly in the North, the depression has an average depth of –0.42 m, is wider and expands deeper towards the open sea, passing the reef through a channel 4 m wide and with a max depth of –0.75 m. In the South, the depression shows a very elongated shape following the inner side of the reef until it becomes parallel to the coast and then goes out from the lagoon through a small channel, 2 m wide and –0.45 m deep (Fig. 12). The depth distribution of the *P. oceanica* upper limit calculated by bathymetry via GIS showed an average value of –0.27 m.

3D reconstruction

By 3D reconstruction, performed matching DEM with photomosaic on the whole area, we could appreciate the 3D image of reef structure and the morphometric information associated (Fig. 13). 3D representation of reef platform showed further details concerning their morphology allowing better understanding of the extension of the reef, from leaf canopy up to landscape scale. This picture gives a real and immersive perception of reef architecture from sea surface to greater depth. For example, particular mor-

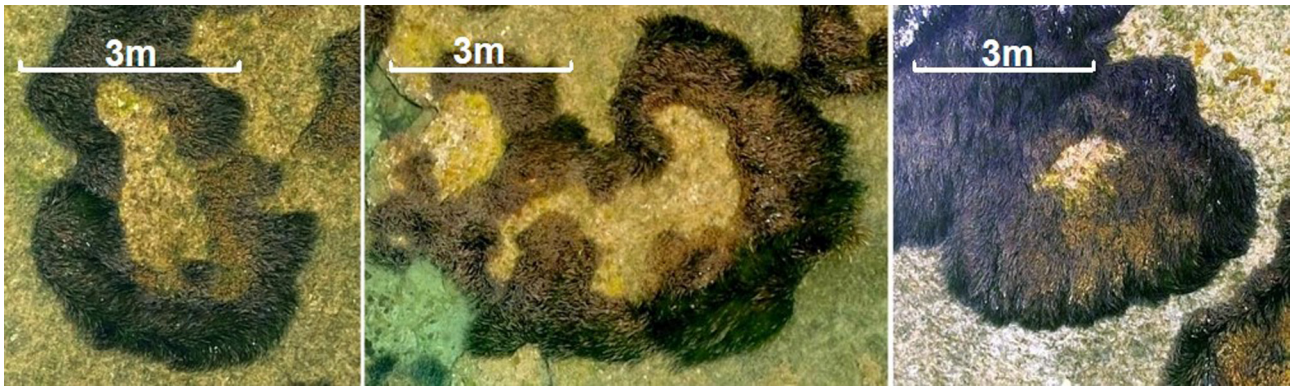

Fig. 9. – Examples of atolls with a multiple arched perimeter. Note how the empty central zone varies in size and shape.

phologies at the boundaries of the reef coincide with the wider channel entering inside the small lagoon reported before (cf. bathymetric map). Some of these boundaries corresponded to dead *matte* wall. Spatial profile from 3D model allowed to estimate *matte* wall thickness ranging from 0.21 to 0.82 m and average value equal to 0.59 m ± 0.20 S.D. (n = 10), while *matte* wall thickness at same point *in situ* ranged from 0.35 m to 1.00 m and

Fig. 10. – Patches of *Posidonia* composed mainly of living shoots.

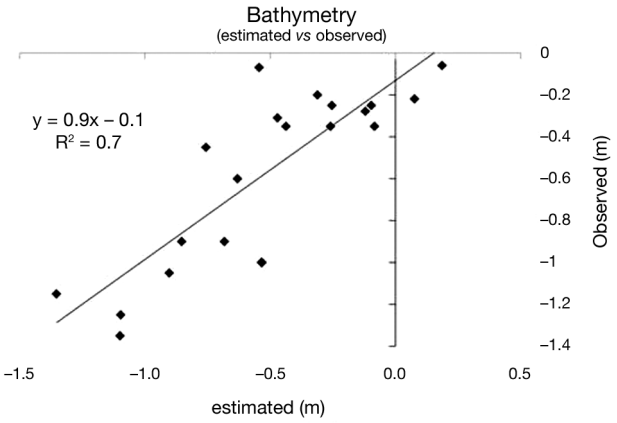

Fig. 11. – Regression between bathymetry recorded *in situ* and estimated through the model.

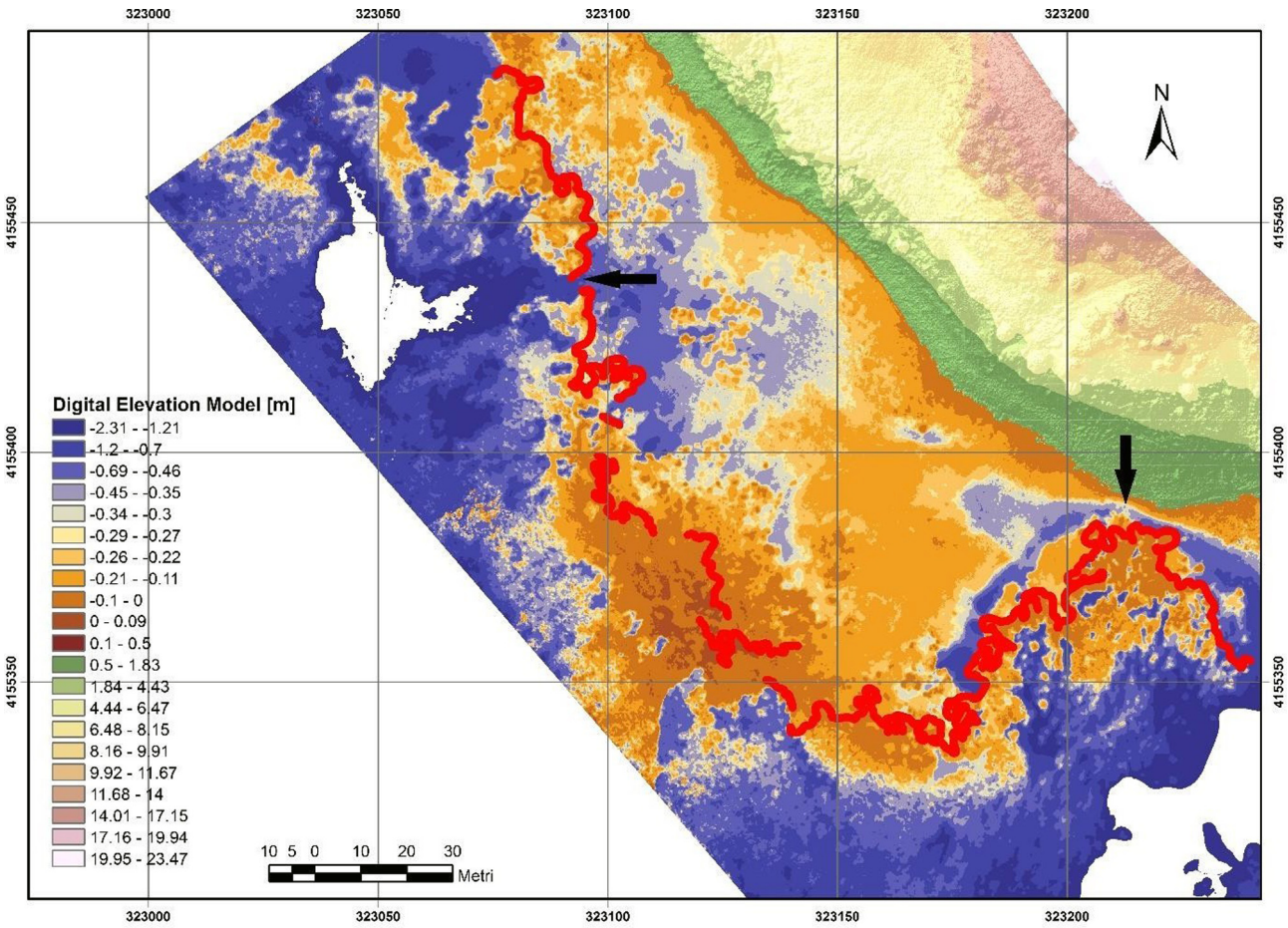

Fig. 12. – Digital elevation model of the area. Red lines and black arrows indicate *P. oceanica* upper limit and the two channels, respectively.

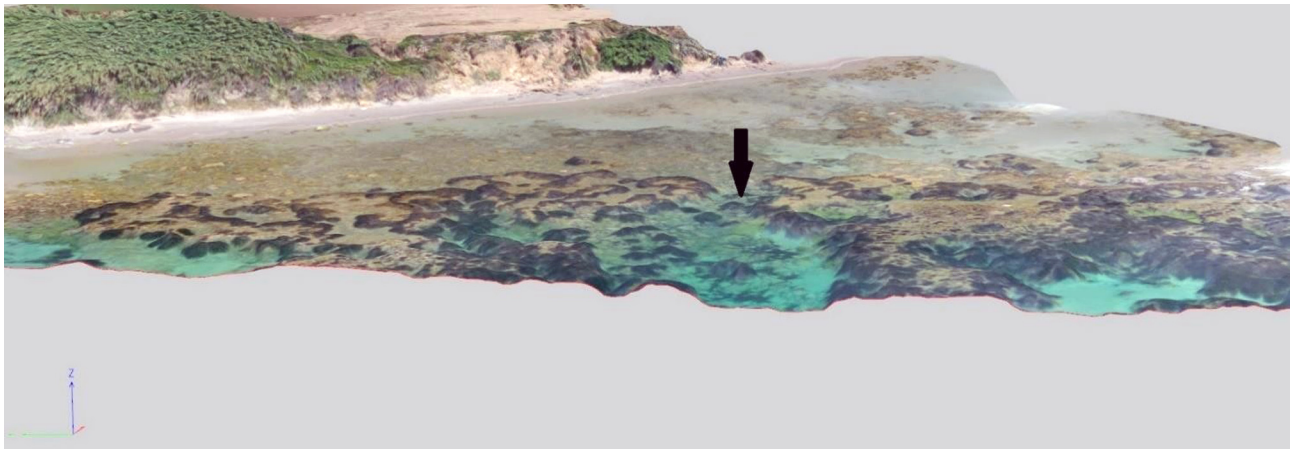

Fig. 13. – 3D-model of the *P. oceanica* reef; the arrow indicates the northern channel.

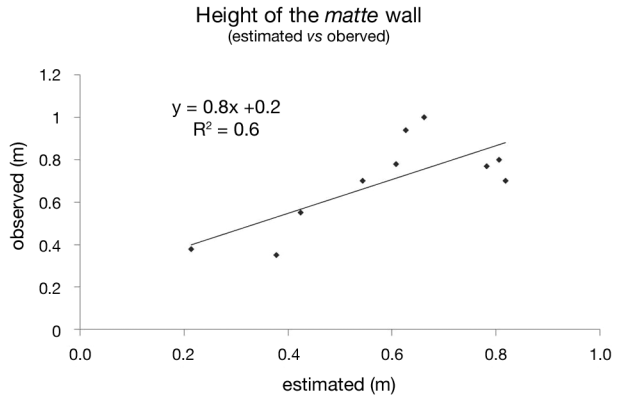

Fig. 14. – Regression between dead *matte* thickness recorded *in situ* and estimated via the 3D-model.

average value equal to 0.70 m ± 0.22 SD (Fig. 14). On the basis of these results the error of mean *matte* wall thickness estimate was –15.9 %.

DISCUSSION AND CONCLUSION

Our study showed that it is possible to analyze *Posidonia oceanica* reefs by using very high-resolution images acquired from drones. The approach used has also highlighted the potential of this method to obtain 3D representation of reefs. This was allowed because seabed was clearly visible through the water surface, and with further processing it was possible to quantify bathymetry via digital terrain models (DTMs) (Ventura *et al*. 2018). Traditionally, high-resolution bathymetry maps have been successfully obtained by gathering high-resolution seabed MBS data in shallow and deep waters (Di Maida *et al*. 2011). However, such device cannot be used in very shallow water (less than 50 cm) due to multiple acoustic reflections between the sea surface and the seabed resulting in a significant noise, heavily affecting the beam signal. Our results provide evidence that UAVs are a very simple and, at the same time, cheap solution able to represent not only seagrass 2D distribution, but also its 3D architecture at a small spatial scale in a very high heterogeneous environment, similarly to what has already been achieved in meadows at greater depths through passive (Rende *et al*. 2015, Ventura *et al*. 2018), or active remote sensing methodologies (Komatsu *et al*. 2003, Di Maida *et al*. 2011). The 2D seagrass distribution combined with DEM model gave, indeed, a very accurate bathymetrical distribution of *Posidonia* reefs, which in this specific case represent the upper limit of the species in the area. The natural upper limit of *P. oceanica* settled on sand or other soft bottoms and on *matte* can be predicted on the basis of physical parameters, which, in a large-scale study carried out along the Mediterranean coasts, was estimated to occur at depths greater than 3.2 m (Montefalcone *et al*. 2019). Only in presence of rocky substrates, the upper limit can be considerably shallower due to the ability of rhizomes to anchor tenaciously, thus allowing the plant to endure the hydrodynamic forces (Montefalcone *et al*. 2016). This is our case, since shoots are settled directly, or through a thin *matte* layer, on rocky outcrops or stones corroborating the statement emphasized by Calvo *et al*. (1995) and Badalamenti *et al*. (2015), that the distribution, settlement and development of *P. oceanica* meadows often coincide with the occurrence of this kind of substrate, because of the peculiar traits of the root system, which enhances the mechanical properties of the plants (Badalamenti *et al*. 2015, Balestri *et al*. 2015, Tomasello *et al*. 2018, Zenone *et al*. 2020).

The resolution of drone acquisition was so high that allowed the estimation of other features of the reef, such as the distribution of surrounding dead *matte* and its thickness, which in some points reached 1 m. To our knowledge, this is the first time that such data have been obtained through aerial images, giving the opportunity to estimate not only the distribution of the foliar canopy, but also of the dead hypogeal component represented by dead *matte*. Although these estimates were possible

for only the emerging and visible portions of the *matte*, which sometimes can be much extended vertically below the bottom (Lo Iacono *et al*. 2008, Tomasello *et al*. 2009, Monnier *et al*. 2019), the typology of data obtained may have relevant implications on the implementation of the methodology required for better estimating these biogenic structures and consequently the ecosystem services they provide. Indeed, one of the most important values of the *P. oceanica* ecosystem is represented by the vast long-term carbon stock accumulated over millennia within the *matte* (Mateo *et al*. 2006). In reef areas where *P. oceanica* meadows regressed and the leaf canopy disappeared, the underlying *matte* is no longer protected against erosion by high-energy waves (Boudouresque *et al*. 2012). Surveys carried out with the same methodology as that adopted in the present study will therefore allow repeated *matte* thickness measurements in order to improve global estimates of Mediterranean seagrass Blue Carbon sinks and to highlight eventual erosion phenomena, as urgently recommended by the scientific community (Pergent *et al*. 2014).

The use of very high-resolution images made it also possible to identify atoll-like formations. These structures have been observed in small areas of the Mediterranean Sea, along the Tunisian, Turkish and Corsican coasts (Blanpied *et al*. 1979, Boudouresque *et al*. 1990, Pasqualini *et al*. 1995), and in Sicily, so far, exclusively at the Stagnone di Marsala, a lagoon-like coastal basin on the Eastern coast (Calvo & Fradà Orestano 1984). The results of the present study indicate that atoll formations may be more frequent than previously thought. Increasing evidences suggest that *Posidonia* atolls are the result of particular dynamics occurred in very shallow meadows, often subjected to stressful conditions where seagrass meadows can live at the extreme of their environmental tolerance (La Loggia *et al*. 2004, Tomasello *et al*. 2009). Pergent & Pergent-Martini (1995) and Boudouresque *et al*. (2012) hypothesized that atolls origin from nearly circular patches of *P. oceanica*, where plagiotropic (horizontal) shoots only grow outwards, whereas the shoots on the central portion of the patch die. Notoriously, *P. oceanica* is considered as an 'ecosystem engineer' species, given its ability to affect significantly physical, chemical and biological features of their environment up to determine inhospitable conditions for itself (Boudouresque *et al*. 1975). During *matte* elevation, shoots and leaves can rise up to the sea surface forming small lagoon-like environments, within which the hydrodynamic regime reduces abruptly inducing the increase in temperature and salinity variability in comparison with the adjacent open sea. The atolls detected in this study lie right at the inner edge of the reef and in very shallow waters where water circulation is even more affected by seagrasses, especially at low tide when the canopy can occupy the entire water column (Koch *et al*. 2006). Under this circumstance one important consequence is that hydrodynamic regime (and covariates), considered a prominent factor in shaping seagrass landscape (Bell *et al*. 2006), within seagrass patches located at the inner edge of reefs, falls further down greatly affecting shoot vitality. Continuous measurements of environmental variables (especially temperature and salinity) are clearly necessary to characterize the environment inside the atolls. Another important finding that arose from our analysis is that atolls appear very irregularly shaped. Although spatially explicit models have not yet been developed in a way that would explain such complex patterns (Duarte *et al*. 2006), a new hypothesis can explain the phenomenon underlying atoll formations. In a diachronic study, Bonacorsi *et al*. (2013) observed that atolls origin and develop from a single self-maintaining patch, more or less regularly shaped across time. However, this model does not support the complexity of atolls recorded in the present study, where, indeed, atolls appear to be rather elongated in shape or with multiple arcs of different amplitude delimiting their contours. According to Bonacorsi *et al*. (2013), such morphological complexity may be explained only assuming a very variable speed of horizontal growth of the rhizomes placed at the periphery of the patches. Alternatively, a new hypothesis on atolls formation can be formulated, by considering such structures as the results of the union of several patches that came into contact during clonal expansion, still maintaining the geometric memory of their union for a certain time interval. Previous studies carried out along Sicilian coasts seem to support the multi-patch origin here hypothesized, since the genetic structure of atolls was demonstrated to be composed by multiple clones (Tomasello *et al*. 2009).

The *P. oceanica* reef model here presented, obtained by integrating a large amount of extremely accurate photographic data and derived bathymetry, allowed to realize a 3D reconstruction with great realism. The results obtained made it possible to graphically reproduce a spatially heterogeneous mosaic with accuracy unthinkable a few years ago. The devices here employed are being continuously implemented in terms of miniaturization and lightening of vehicles, sensor resolution and powerful softwares. Surely the advent of these technologies represents the beginning of a new era in the study and monitoring of these important natural monuments, since many of the limitations of classical methods applied at seagrass landscape level such as incorrect positioning, low resolution and consequent misleading interpretation of data (Bell *et al*. 2006), may now be considered overcome.

ACKNOWLEDGEMENTS. – This study was supported by the project Pocket Beach Management & Remote Surveillance System (BESS) Interreg Italia-Malta funded by European Union.

REFERENCES

Agrafiotis P, Karantzalos K, Georgopoulos A, Skarlatos D 2020. Correcting image refraction: towards accurate aerial image based bathymetry mapping in shallow waters. *Remote Sens* 12(2): 322.

Anderson K, Gaston KJ 2013. Lightweight unmanned aerial vehicles will revolutionize spatial ecology. *Front Ecol Environ* 11(3): 138-146.

Badalamenti F, Alagna A, Fici S 2015. Evidences of adaptive traits to rocky substrates undermine paradigm of habitat preference of the Mediterranean seagrass *Posidonia oceanica*. *Sci Rep* 5: 8804.

Balestri E, De Battisti D, Vallerini F, Lardicci C 2015. First evidence of root morphological and architectural variations in young *Posidonia oceanica* plants colonizing different substrate typologies. *Estuar Coast Shelf Sci* 154: 205-213.

Bell SS, Fonseca MS, Stafford NB 2006. Seagrass ecology: new contributions from a landscaper perspective. *In* Larkum AWD, Orth RJ, Duarte CM Eds, Seagrasses: Biology, Ecology and Conservation. Springer Netherlands: 625-645.

Blanpied C, Burollet PF, Clairefond P, Shimi M 1979. Sédiments actuels et holocènes. *In* La Mer pélagienne : Étude sédimentologique et écologique du Plateau tunisien et du Golfe de Gabès. *Geol Medit* 6(1): 61-82.

Bonacorsi M, Pergent-Martini C, Breand N, Pergent G 2013. Is *Posidonia oceanica* regression a general feature in the Mediterranean Sea? *Medit Mar Sci* 14(1): 193-203.

Boudouresque CF, Meinesz A 1982. Découverte de l'herbier de posidonie. *Cah Parc Natl Port-Cros*, v. 4.

Boudouresque CF, Augier H, Belsher T, Coppejans E, Perret M 1975. Végétation marine de l'île de Port-Cros (parc national). X. La régression du récif-barrière de posidonies. *Trav Sci Parc Natl Port-Cros* 1: 41-46.

Boudouresque CF, Ballesteros E, Ben Maiz N, Boisset F, Bouladier E, Cinelli F, Cirik S, Cormaci M, Jeudy de Grissac A, Laborel J, Lanfranco E, Lundberg B, Mayhoub H, Meinesz A, Panayotidis P, Semroud R, Sinnassamy JM, Span A, Vuignier G 1990. Livre rouge 'Gérard Vuignier' des végétaux, peuplements et paysages marins menacés de Méditerranée. PNUE, Aires Spécialement Protégées: 250 p.

Boudouresque CF, Bernard G, Bonhomme P, Charbonnel E, Diviacco G, Meinesz A., Pergent G, Pergent- Martini C, Ruitton S, Tunesi, L 2012. Protection and conservation of *Posidonia oceanica* meadows. RAMOGE and RAC/SPA, Tunis: 1-202.

Boudouresque CF, Pergent G, Pergent-Martini C, Ruitton S, Thibaut T, Verlaque M 2016. The necromass of the *Posidonia oceanica* seagrass meadow: fate, role, ecosystem services and vulnerability. *Hydrobiologia* 781(1): 25-42.

Boussard A, Barralon E, Boudouresque CF, Boursault M, Goujard A, Pergent G, Pergent-Martini C, Rouanet E, Schohn T 2019. Almost a century of monitoring of the *Posidonia* barrier reef at Port-Cros (Provence) and the platform reef at Saint-Florent (Corsica). *In* Proc Langar H, Ouerghi A Eds, 6th Medit Symp on Marine Vegetation, Antalya, Turkey, 14-15 January 2019. SPA/RAC, Tunis: 41-46.

Buia MC, Gambi MC, Zupo V 2000. Structure and functioning of Mediterranean seagrass ecosystem: an overview. *Biol Mar Medit* 7(2): 167-190.

Calvo S 1987. Un Monumento naturale: lo Stagnone. Le Provincie Siciliane – Trapani. Ediprint.

Calvo S, Fradà Orestano C 1984. L'herbier de *Posidonia oceanica* des côtes siciliennes : les formations récifales du Stagnone. *In* Boudouresque CF, Jeudy de Grissac A, Olivier J Eds, International Workshop on *Posidonia oceanica* Beds. GIS Posidonie 1: 29-37.

Calvo S, Fradà Orestano C, Tomasello A 1995. Distribution, structure and phenology of *Posidonia oceanica* meadows along Sicilian coasts. *Giorn Bot Ital* 129(1): 351-356.

Casella E, Collin A, Harris D, Ferse S, Bejarano S, Parravicini V, Hench L, Rovere A 2017. Mapping coral reefs using consumer-grade drones and structure from motion photogrammetry techniques. *Coral Reefs* 36(1): 269-275.

Caye G 1980. Analyse du polymorphisme caulinaire chez *Posidonia oceanica* (L.) Del *Boll Soc Bot Fr Lett* 127(3): 257-262.

Caye G 1982. Étude sur la croissance de la Posidonie, *Posidonia oceanica* (L.) Delile, formation des feuilles et croissance des tiges au cours d'une année. *Téthys* 10: 229-235.

Di Maida G, Tomasello A, Luzzu F, Scannavino A, Pirrotta M, Orestano C, Calvo S 2011. Discriminating between *Posidonia oceanica* meadows and sand substratum using multibeam sonar. *ICES J Mar Sci* 68(1): 12-19.

Duarte CM, Fourqurean J W, Krause-Jensen D, Olesen B 2006. Dynamics of seagrass stability and change. *In* Larkum AWD, Orth RJ, Duarte CM Eds, Seagrasses: Biology, Ecology and Conservation. Springer Netherlands 26: 271-94.

Duffy JP, Shutler JD, Witt MJ, DeBell L, Anderson K 2018. Tracking fine scale structural changes in coastal dune morphology using kite aerial photography and uncertainty-assessed structure-from-motion photogrammetry. *Remote Sens* 10(9): 1494.

Figueira W, Ferrari R, Weatherby E, Porter A, Hawes S, Byrne M 2015. Accuracy and precision of habitat structural complexity metrics derived from underwater photogrammetry. *Remote Sens* 7(12): 16883-16900.

Francour P, Ganteaume A, Poulain M 1999. Effects of boat anchoring in *Posidonia oceanica* seagrass beds in the Port-Cros National Park (north-western Mediterranean Sea). *Aquat Conserv* 9(4): 391-400.

Hemminga MA, Duarte CM 2000. Seagrass Ecology. Cambridge University Press. 289 p.

IPCC 2019. Summary for Policymakers. *In* Pörtner HO, Roberts DC, Masson-Delmotte V, Zhai P, Tignor M, Poloczanska E, Mintenbeck K, Nicolai M, Okem A, Petzold J, Rama B, Weyer N Eds, IPCC Special Report on the Ocean and Cryosphere in a Changing Climate. In press.

Jeudy de Grissac A, Boudouresque CF 1985. Rôles des herbiers de phanérogames marines dans les mouvements des sédiments côtiers : les herbiers à *Posidonia oceanica*. Les aménagements côtiers et la gestion du littoral. *Coll Pluridisciplinaire Franco-Jpn Océanogr*: 143-151.

Koch EW, Ackerman JD, Verduin J, van Keulen M 2006. Fluid dynamics in seagrass ecology – from molecules to ecosystems. *In* Larkum AWD, Orth RJ, Duarte CM. Eds, Seagrasses: Biology, Ecology and Conservation. Springer Netherlands, 26: 193-225.

Komatsu T, Igarashi C, Tatsukawa K, Sultana S, Matsuoka Y, Harada S 2003. Use of multi-beam sonar to map seagrass beds in Otsuchi Bay on the Sanriku Coast of Japan. *Aquat Living Res* 16: 223-230.

La Loggia G, Calvo S, Ciraolo G, Mazzola A, Pirrotta M, Sarà G, Tomasello A, Vizzini S 2004. Influence of hydrodynamic conditions on the production and fate of *Posidonia oceanica* in a semi-enclosed shallow basin (Stagnone di Marsala, Western Sicily). *Chem Ecol* 20(3): 183-201.

Lo Iacono C, Mateo MA, Gracia E, Guasch L, Carbonell R, Serrano L, Danobeitia J 2008. Very high-resolution seismoacoustic imaging of seagrass meadows (Mediterranean Sea): implications for carbon sink estimates. *Geophys Res Lett* 35(18): L18601.

Marre G, Holon F, Luque S, Boissery P, Deter J 2019. Monitoring marine habitats with photogrammetry: a cost-effective, accurate, precise and high-resolution reconstruction method. *Mar Sci* 6: 276.

Mateo MA, Romero J, Pérez M, Littler MM, Littler DS 1997. Dynamics of millenary organic deposits resulting from the growth of the Mediterranean seagrass *Posidonia oceanica*. *Estuar Coast Shelf Sci* 44(1): 103-110.

Mateo MA, Cebrìan J, Dunton K, Mutchler T 2006. Carbon flux in seagrass ecosystem. *In* Larkum AWD, Orth RJ, Duarte CM Eds, Seagrasses: Biology, Ecology and Conservation. Springer Netherlands, 7: 159-192.

Mazzella L, Buia MC 1986. Strategie evolutive nelle fanerogame marine del Mediterraneo. *Nov Thalassia* 8: 651.

Mazzella L, Buia MC, Gambi MC, Lorenti M, Russo GF, Scipione MB, Zupo V 1992. Plant-animal trophic relationships in the *Posidonia oceanica* ecosystem of the Mediterranean Sea: a review. *In* John DM, Hawkins SJ, Pric JH Eds, Plant-animal Interactions in Marine Benthos. Clarendon Press: 65-187.

Molinier R, Picard J 1952. Recherches sur les herbiers de phanérogames marines du littoral méditerranéen français. *Ann Inst Océanogr* 27: 208-234.

Monnier B, Clabaut P, Mateo MA, Pergent-Martini C, Pergent G 2019. Intercalibration of seismic reflection data and characterization of *Posidonia oceanica* meadow mats. *In* Langar H, Ouerghi A Eds, Proceedings 6th Medit Symp on Marine Vegetation, Antalya, Turkey, 14-15 January 2019. SPA/RAC, Tunis: 68-73.

Montefalcone M, Chaintore M, Lanzone A, Morri C, Albertelli G, Bianchi CN 2008. BACI design reveals the decline of the seagrass *Posidonia oceanica* induced by anchoring. *Mar Pollut Bull* 56(9): 1637-1645.

Montefalcone M, Vacchi M, Carbone C, Cabella R, Schiaffino CF, Elter FM, Morri C, Bianchi CN, Ferrari M 2016. Seagrass on the rocks: *Posidonia oceanica* settled on shallow-water hard substrata withstands wave stress beyond predictions. *Estuar Coast Shelf Sci* 180: 114-122.

Montefalcone M, Vacchi M, Archetti R, Ardizzione G, Astruch P, Bianchi CN, Calvo S, Criscoli A., Fernández-Torquemada Y, Luzzu F, Misson G, Morri C, Pergent G, Tomasello A, Ferrari M 2019. Geospatial modeling and map analysis allowed measuring regression of the upper limit of *Posidonia oceanica* seagrass meadows under human pressure. *Estuar Coast Shelf Sci* 217: 148-157.

Pasqualini V, Pergent-Martini C, Pergent G 1995. Etude de la formation récifale de Saint-Florent (Haute-Corse). Cartographie et évolution. Contrat DIREN/GIS Posidonie, GIS Posidonie: 49 p.

Pergent G, Pergent-Martini C 1995. Dynamique et évolution de l'herbier à *Posidonia oceanica* en Méditerranée. *Plant Biosyst* 129(1): 303-317.

Pergent G, Djellouli A, Hamza AA, Ettayeb KS, Alkekli A, Talha M, Alkunti E 2007. Structure of *Posidonia oceanica* meadows in the vicinity of Ain Al-Ghazala lagoon (Libya): the "macroatoll" ecomorphosis. *In* Pergent-Martini C, El Asmi S, Le Ravallec C Eds, Proc third Medit Symposium on Marine Vegetation, Marseille, 27-29 March 2007. RAC/SPA, Tunis: 135-140.

Pergent G, Bazairi H, Bianchi CN, Boudouresque CF, Buia MC, Calvo S, Clabaut P, Harmelin-Vivien M, Mateo MA, Montefalcone M, Morri C, Orfanidis S, Pergent-Martini C, Semroud R, Serrano O, Tomasello A, Verlaque M 2014. Climate change and Mediterranean seagrass meadows: a synopsis for environmental managers. *Medit Mar Sci* 15(2): 462-473.

Perzia P, Falautano M, Castriota L, Cillari T, Vivona P, Toccaceli M, Scotti G, Andaloro F 2011. Indagine geomorfologica e bionomica dei fondali di Sciacca (AG). *Biogeogr J Integr Biogeogr* 30(1).

Rende FS, Irving AD, Lagudi A, Bruno F, Scalise S, Cappa P, Montefalcone M, Bacci T, Penna M, Trabucco B, Di Mento R, Cicero AM 2015. Pilot application of 3D underwater imaging techniques for mapping *Posidonia oceanica* (L.) Delile meadows. *Int Arch Photogr Remote Sens Spat Inf Sci* 40(5): 177.

Rouanet E, Goujard A, Barralon E, Boudouresque CF, Boursault M, Boussard A, Larroudé P, Meulé S, Paquier AE, Pergent-Martini C, Pergent G, Schohn T 2019. Inventory and mapping of *Posidonia oceanica* reefs of the French Mediterranean coast. *In* Langar H, Ouerghi A Eds, Proc 6th Medit Symp on Marine Vegetation, Antalya, Turkey, 14-15 January 2019. SPA/RAC, Tunis: 129-130.

Short FT, Neckles HA 1999. The effects of global climate change on seagrasses. *Aquat Bot* 63(3-4): 169-196.

Tomasello A, Di Maida G, Calvo S, Pirrotta M, Borra M, Procaccini G 2009. Seagrass meadows at the extreme of environmental tolerance: the case of *Posidonia oceanica* in a semi-enclosed coastal lagoon. *Mar Ecol* 30(3): 288-300.

Tomasello A, Perrone R, Colombo P, Pirrotta M, Calvo S 2018. Root hair anatomy and morphology in *Posidonia oceanica* (L.) Delile and substratum typology: first observations of a spiral form. *Aquat Bot* 145: 45-48.

Ventura D, Bonifazi A, Gravina MF, Belluscio A, Ardizzone G 2018. Mapping and classification of ecologically sensitive marine habitats using unmanned aerial vehicle (UAV) imagery and object-based image analysis (OBIA). *Remote Sens* 10(9): 1331.

Vizzini S 2009 Analysis of the trophic role of Mediterranean seagrasses in marine coastal ecosystems: a review. *Bot Mar* 52: 383-393.

Woodget AS, Carbonneau PE, Visser F, Maddock IP 2015. Quantifying submerged fluvial topography using hyperspatial resolution UAS imagery and structure from motion photogrammetry. *Earth Surf Proc* 40(1): 47-64.

Zenone A, Alagna A, D'Anna G, Kovalev A, Kreitschitz A, Badalamenti F, Gorb SN 2020. Biological adhesion in seagrasses: The role of substrate roughness in *Posidonia oceanica* (L.) Delile seedling anchorage via adhesive root hairs. *Mar Environ Res* 160: 105012.